Modelling of an Embankment Failure Using Flow-3D

M. Y. Zainab, A. L. S. Zebedee, A. W. Ahmad Khairi, I. Zulhilmi, and A. Shahabuddin

Abstract Embankment dam failures are concerning to many people in society today, including dam engineers, federal, state, and local officials. The effects of dam failure will cause more harm than good, leading to the losses of lives, properties being damaged, economic and environmental issues. The embankment dam breaching is a complex process between hydraulics and soil erosion processes that requires an analysis of hydrodynamic parameters such as breach outflow hydrograph, peak outflow rate and failure time, and geometric parameters; breach depth, H_b, and top breach width, B_t. . With the aid of simulation techniques such as Computational Fluid Dynamics (CFD), it is possible to understand the behaviour of embankment breaching processes. In this paper, modelling of an embankment breaching using FLOW-3D allows modellers to open doors to plenty of experiments to breaching in the near future. This paper focuses on analyzing the modelling breaching embankment for different sediment sizes of embankment material to investigate the patterns of breached outflow, breach width, dam breach depth. Moreover, the study also investigates the hydrostatic pressure, free surface elevation and shear stress on embankment during the breaching failure processes.

M. Y. Zainab (✉)
Eco-Hydrology, School of Civil Engineering, Faculty of Engineering, Universiti Teknologi Malaysia, Johor Bahru, Malaysia
e-mail: zainabyusof@utm.my

A. L. S. Zebedee
School of Civil Engineering, Faculty of Engineering, Universiti Teknologi Malaysia, Johor Bahru, Malaysia

A. W. A. Khairi · I. Zulhilmi
Centre for River and Coastal Engineering (CRCE), Faculty of Engineering, Universiti Teknologi Malaysia, Johor Bahru, Malaysia
e-mail: akhairi@utm.my

I. Zulhilmi
e-mail: zulhilmi@utm.my

A. Shahabuddin
Department of Geoinformation, Faculty of Built Environment and Surveying, Universiti Teknologi Malaysia, Johor Bahru, Malaysia
e-mail: shahabuddin@utm.my

1 Introduction

Dam failures, either from accidents or deliberate acts, may cause disastrous damage towards downstream areas. Major flood waves brought by the dam failure may cause serious damage or destroy industrial or power plants, houses and bridges; transportation, navigation, irrigation and social economy activities; and may cause loss of life, spoiling of agricultural land, and adversity of ecological and environmental impacts.

According to [1], approximately 34% of dam failures are caused by overtopping, 30% by foundation defects, and 28% by piping. Overall, the most common causes of embankment failure are overtopping and internal erosion. [5] indicates that there are approximately 57 000 dams in the United States that have the potential for overtopping. In obtaining breach parameters from regression analysis, [6] stated dam erodibility plays a significant role in influencing the results of breaching parameters. Sand has high erodibility compared to clay which has low erodibility, and hence higher resistance to fast-moving water.

Data collected by the Association of State Dam Safety Officials (ASDSO, 2020) between 2010 and 2019 showed that dam failure by overtopping ranked the highest for a number of incidents and followed by piping. Overtopping is caused when water spills over the top of the dam and causes erosions. Overtopping may occur due to inadequacy of spillway design, blockage by debris at the spillway, or settlement of the dam crest.

Overtopping is a result of insufficient spillway capacity or an event of extreme rainfall, which causes the water level to exceed design criteria. The water flow over the embankment from overtopping introduces tractive shear stress on the downstream surface [4]. The erosion process begins at a weak spot where the tractive shear stress exceeds a critical resistance that keeps the soil material in place [3, 7]. The process will continue under the action of flowing water while soil materials are being transported downstream. The initial breach is often V-shaped and becomes larger as the erosion progresses, which finally results in an inverse trapezoidal shape. The extent of breaching usually depends on the duration of overtopping and the structure of the embankment. In fact, the erosion characteristics are different for granular and cohesive embankments. Granular soil is non-cohesive soil such as sand or small gravel, whereas an example of cohesive soil is clay.

For non-cohesive embankments, the overtopping flow of water on downstream slope causes surface slip to take place quickly, hence resulting in non-cohesive materials to be removed rapidly, layer by layer. Usually, the end result for breaching in this manner tends to become flattened, depending upon the material and the longitudinal slope of the foundation surface. For cohesive embankments, erosion often starts at the embankment toe and advances upstream, undercutting the slope and in turn causing the removal of large chunks of materials due to tensile or shear failure of the soil on the over-steepened slope. In certain cases, a series of stair-step head-cuts develop at the downstream face.

2   Breaching Embankment Modelling

In this study, FLOW-3D v11.2 [2], which was developed by Flow Science, Inc. USA, is used to investigate the breaching processes to analyse the breaching parameters such as shear stress, hydrostatic pressure and free surface elevation. The output of breaching outflow hydrographs and comparison of sediment sizes of the embankment is also modelled to predict the breach patterns and breach outflows.

The embankment is modelled using AutoCad 3D before importing into FLOW-3D for meshing generation. Figure 1 shows the geometry of the embankment and the model setup. The model setup has a total channel length of 12 m with upstream and downstream lengths of 8.5 and 1.815 m, respectively. A structured and uniform mesh size of 0.02 m is used where the finer mesh is located in the embankment area to get more accurate simulation results.

The simulation was run for 400 s using the sediment scour physical model. The embankment sediment was set to be 0.1 (fine), 0.4 (medium) and 0.8 mm (coarse) with an inflow rate of 0.012 m^3/s. The initial state of the solution for transient fluid flow problems must be known in order to find a solution and, in a manner similar to what is done with boundary conditions, the initial conditions are assumed, approximating the true state at time $t = 0$. The Boundary conditions used are Volume Flow Rate (Q), Outflow (O), Symmetry (S), Wall (W) and Specified pressure (P), and the location to apply the boundary conditions is shown in Fig. 2.
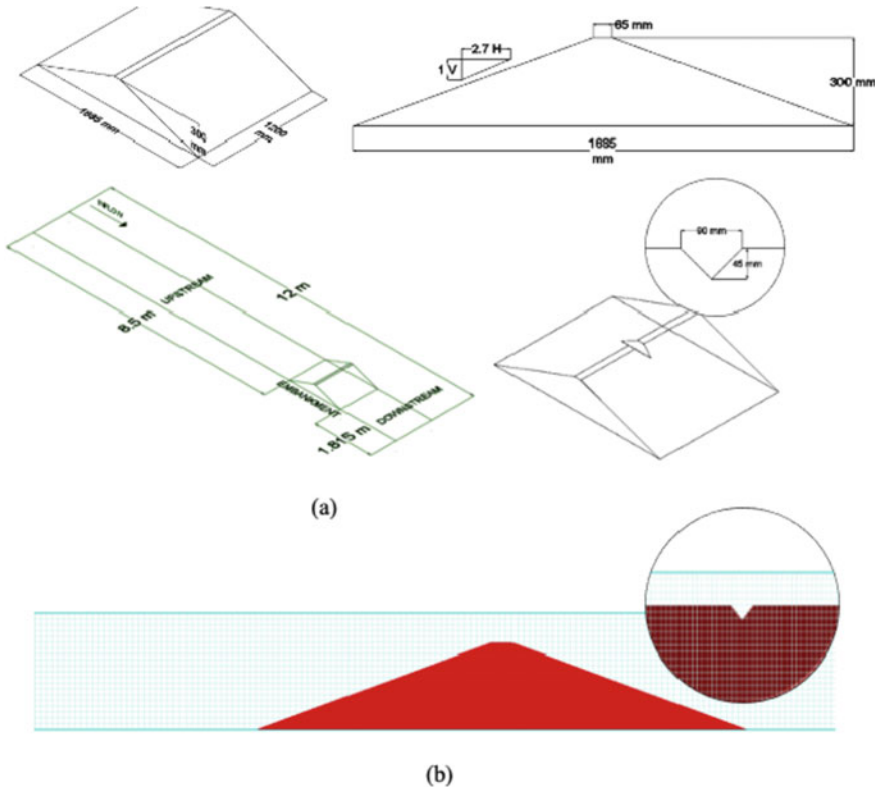
(a)

(b)

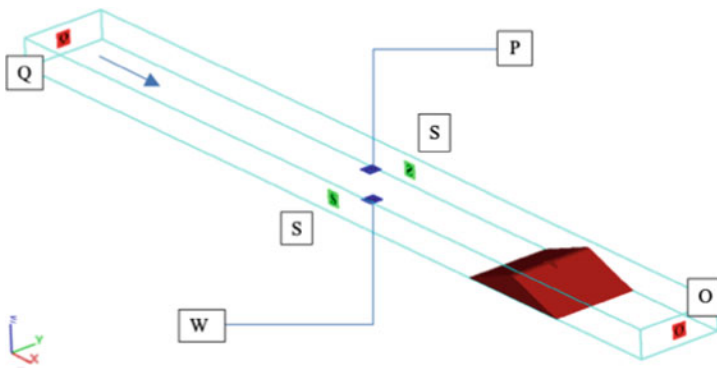**Fig. 1** Model setup **a** Embankment geometry, and **b** Meshing size

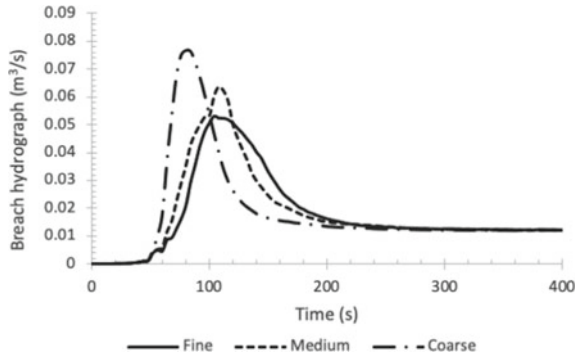**Fig. 2** Boundary conditions of the model setup

Fig. 3 Breach outflow hydrograph for different sediment sizes

3 Results and Discussions

The modelling of breaching embankment with different sizes of sediments diameter showed that the breaching occurs slower when the sediment is finer as compared to larger sediment embankments. This is because the fine sand seems to be more resistant to erosion. Figure 3 shows the peak outflow hydrograph for coarse sand with a diameter of 0.8 mm is 0.0768 m^3/s, and for fine sand with a diameter of 0.1 mm, the peak is 0.0532 m^3/s. The outflow hydrograph is measured at the outlet of the channel where the v-notch is installed. Meanwhile, for medium sand with a diameter of 0.4 mm, the peak outflow hydrograph is 0.0638 m^3/s. As for the failure time where the breaching started, the coarse sand obtained a failure time of 80 s, while that of the fine sand had a failure time of 104 s. The failure time for the medium sand is 108 s which is almost as similar to the failure time for the fine sand (Fig. 5).

In the breaching process, the flowrate plays an important role in the erosion and scour of the embankment, the widening and deepening process of the breach, and the flood propagation process downstream. Figure 4 illustrates the breach profiles – failure lines patterns with sediment size of 0.4 mm and inflow rate of 0.012 m^3/s at time 40, 60, 80, 100, 120 and 140 s, respectively. As breach depth increases and the height of the embankment reduces, the downstream slope angle of the embankment decreases, as can be observed in Fig. 4. The details of the breach patterns with respect to the free surface profiles and hydrostatic pressure is shown in Fig. 6.
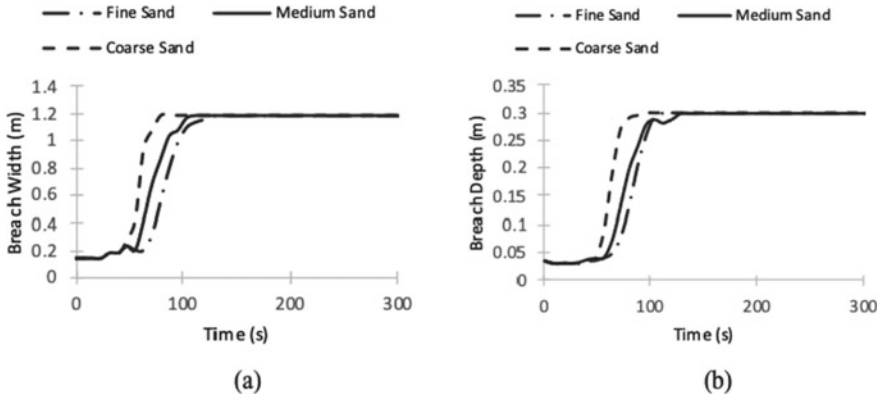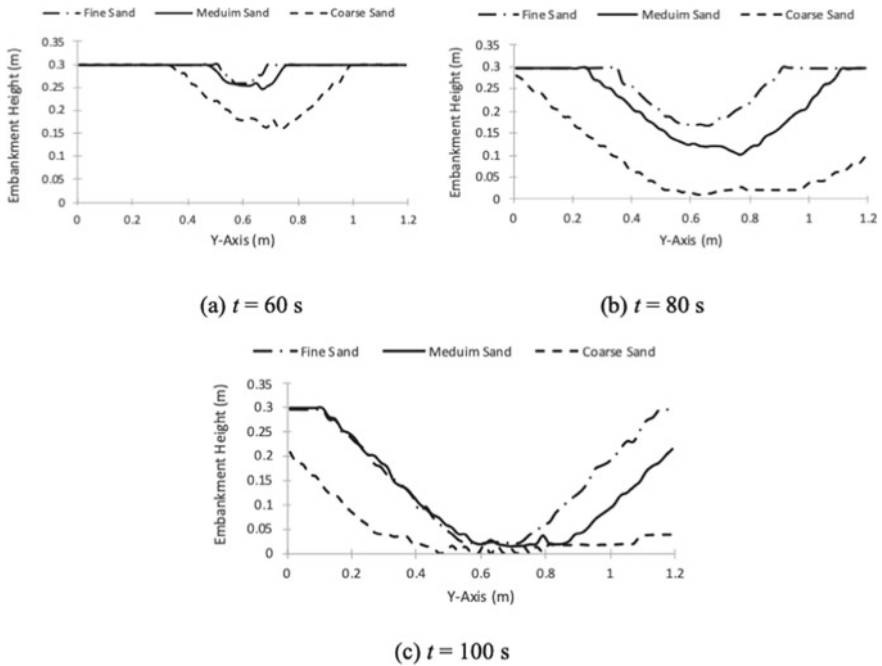
Fig. 4 **a** Breach width and **b** breach depth against time

Fig. 5 Breach growth for **a** $t = 60$, **b** $t = 80$ and **c** $t = 100$ s

Meanwhile, for hydrostatic pressure analysis, there is an increment in bottom pressure from $t = 40$ s to $t = 60$ s. This is due to a rising in water elevation during the overtopping flow. Since the erosion rate at this condition is still slow, the embankment height shows little change, which results in hydraulic jump and an increase in water elevation. At $t = 80$ s, the hydrostatic pressure at the bottom decreases as
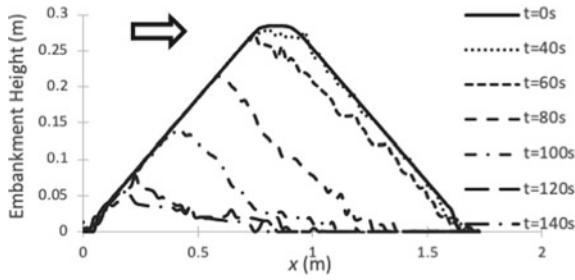
Fig. 6 Progression of breaching profiles at various time intervals

the embankment height decreases due to erosions, from the result of lower water elevation. As the erosion continues, the hydrostatic pressure at the bottom continues to decrease as the embankment height decreases due to erosion. This can be seen at $t = 120$ s to $t = 140$ s. This progression can be observed in Fig. 7 for time intervals of 40, 60, 80, 100, 120, and 140 s.

Meanwhile, the shear stress results of 3D modelling of the embankment are shown in Fig. 8. Through the observation of the 3D model results of shear stress, erosion
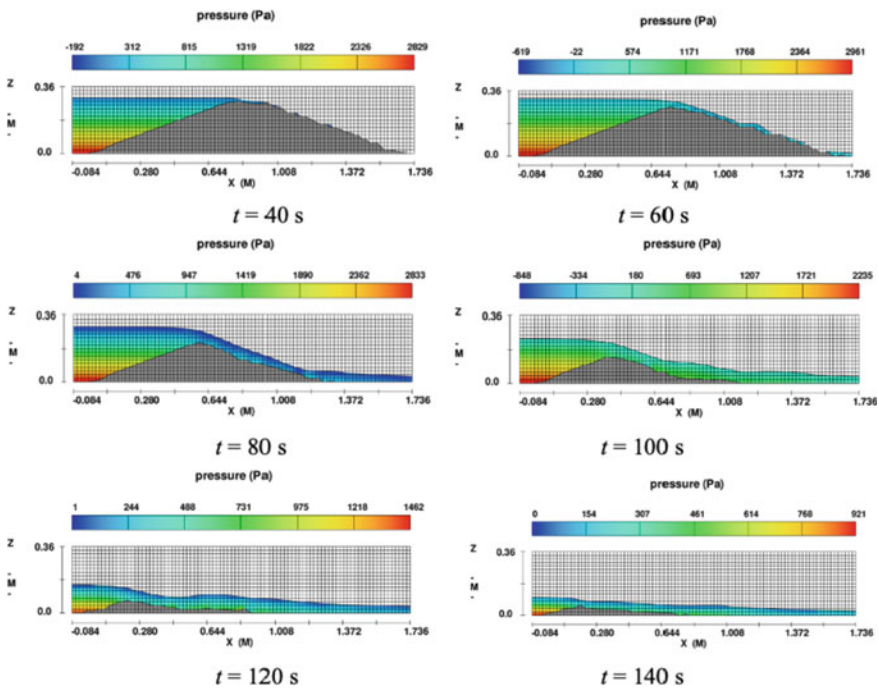
Fig. 7 Changes of free surface elevation with hydrostatic pressure variation during the embankment failure

occurs when shear stress is present. This illustrates how shear stress influences the erosion process in embankment breaching. Also, due to erosion beginning at the canter y-axis of the embankment, the erosion pattern of the embankment resembles a V-shape when looking from a plane view at the embankment downstream.
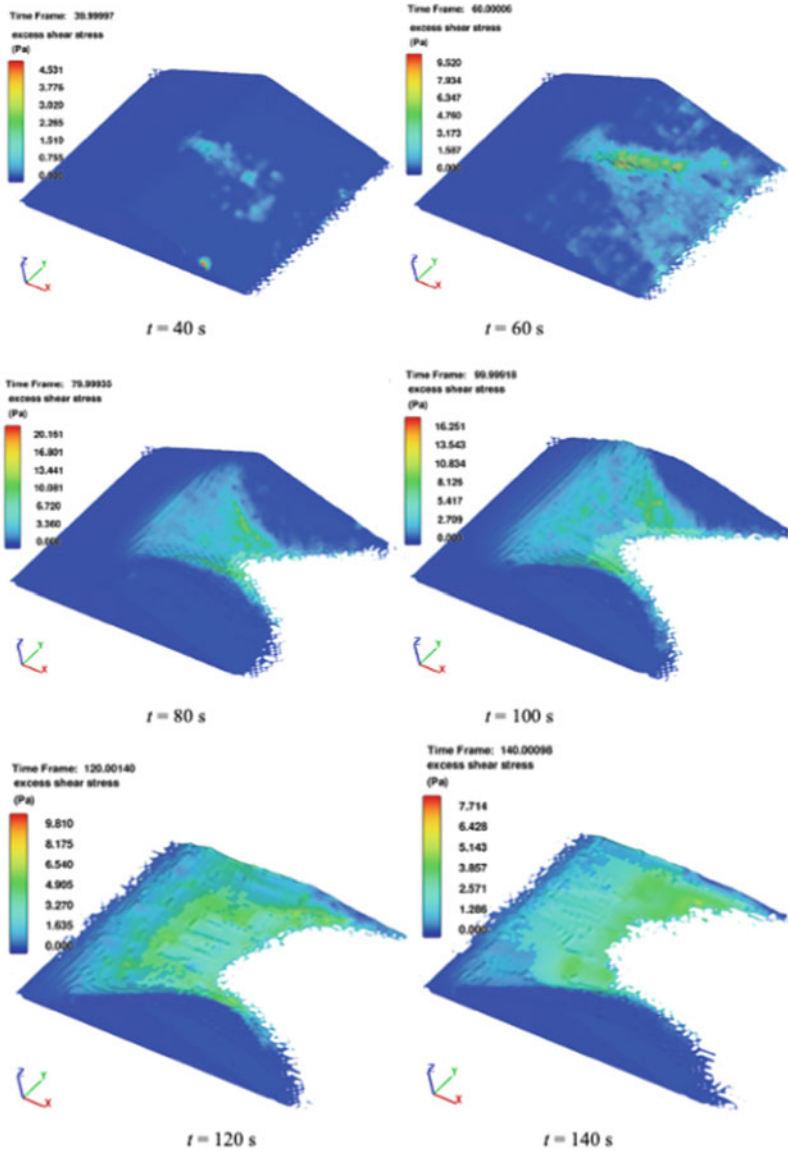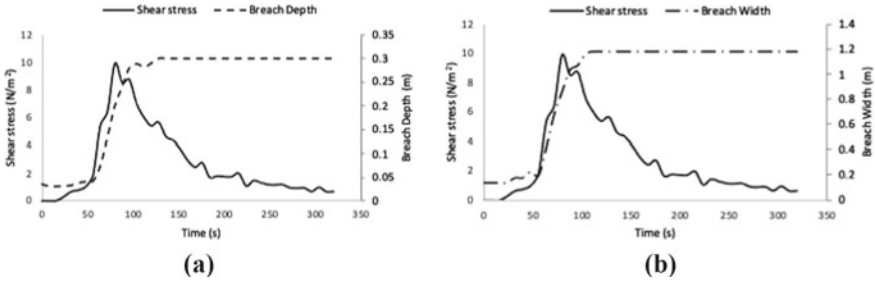

Fig. 8 Shear stress changes of an embankment breaching

Fig. 9 Shear stress against **a** breach depth and **b** breach width

Table 1 Summary of maximum shear stress, breach depth, and top breach width

Time, t (s)	Maximum shear stress, τ (N/m^2)	Breach depth, H_b (m)	Top breach width, B_t (m)
40	0.76	0.04	0.18
60	5.83	0.05	0.31
80	9.87	0.20	0.86
100	8.84	0.28	1.12
120	5.37	0.29	1.18
140	4.51	0.30	1.18

The maximum value of shear stress at cross-section is plotted against time and compared with breach depth and breach width, as shown in Fig. 9. The results indicate an increasing gradient of the curve of the rate of shear stress, the breach depth and the breach width at the beginning of breaching, then slowly, the rate of shear stress starts showing a decreasing gradient. At this point, the breach depth and the breach width hit a constant, reaching their maximum depth and width. Table 1 indicates the summary of the maximum shear stress obtained in relation with breach width and breach depth for $t = 40$ s, $t = 60$ s, $t = 80$ s, $t = 100$ s, $t = 120$ s, and $t = 140$ s.

4   Conclusion

The peak outflow hydrograph is higher and has a shorter failure time for embankment with larger sediment sizes and lower peak outflow hydrograph and longer failure time for embankment with finer sediment sizes. Finer particles are able to provide a greater surface area of contacts between other particles, thus having increased interlocking between soil particles and hence higher resistance to soil erosion. Embankment dams with large sediment sizes will have larger breach depth and width as compared to embankment dams with finer sediment sizes at the end of the breaching process. The breach depth and breach width also show an increment when the shear stress

increases. The shear stress exerted by the flowing water exceeds the critical erosive shear stress of the soil resulting in the erosion of the embankment. The hydrostatic pressure upstream is greater than the hydrostatic pressure downstream. As a result, the surface of the embankment during breaching keeps on eroding and changes shape, which leads to variations in the flow depth.

References

1. Costa JE (1985) Floods from dam failures. Open-File Rep. No. 85-560, USGS, Denver, p 54
2. FLOW-3D (2016) FLOW-3D v11.2 Documentation. Flow Science Inc.
3. Mat Lazin NA (2013) Erodible Dam Breaching Patterns Due to Overtopping. Master thesis, Johor Bahru: Universiti Teknologi Malaysia
4. Powledge GR, Ralston DC, Miller P, Chen YH, Clopper PE, Temple DM (1989) Mechanics of overflow erosion on embankments II: hydraulics and design considerations. J Hydraul Res 115(8):1056–1075
5. Ralston DC (1987) Mechanics of embankment erosion during overflow hydraulic engineering. In: Proceedings of the 1987 National Conference on Hydraulic Engineering, ASCE Reston VA, pp 733–738
6. Xu Y, Zhang LM (2009) Breaching parameters of earth and rockfill dams. J Geotech Geoenviron Eng 135(12):1957–1970
7. Zhao G, Visser PJ, Ren Y, Uijttewaal WSJ (2015) Flow hydrodynamics in embankment breach. J Hydrodyn 27(6):835–844